Precise and Ultrafast Molecular Sieving Through Graphene Oxide Membranes

R. K. Joshi,[1] P. Carbone,[2] F. C. Wang,[3] V. G. Kravets,[1] Y. Su,[1] I. V. Grigorieva,[1] H. A. Wu,[3] A. K. Geim,[1]* R. R. Nair[1]*

Graphene-based materials can have well-defined nanometer pores and can exhibit low frictional water flow inside them, making their properties of interest for filtration and separation. We investigate permeation through micrometer-thick laminates prepared by means of vacuum filtration of graphene oxide suspensions. The laminates are vacuum-tight in the dry state but, if immersed in water, act as molecular sieves, blocking all solutes with hydrated radii larger than 4.5 angstroms. Smaller ions permeate through the membranes at rates thousands of times faster than what is expected for simple diffusion. We believe that this behavior is caused by a network of nanocapillaries that open up in the hydrated state and accept only species that fit in. The anomalously fast permeation is attributed to a capillary-like high pressure acting on ions inside graphene capillaries.

Porous materials with a narrow distribution of pore sizes, especially in the angstrom range (*1*–*5*), are of interest for use in separation technologies (*5*–*7*). The observation of fast permeation of water through carbon nanotubes (*8*–*10*) and, more recently, through graphene-oxide (GO) laminates (*11*) has led to many proposals to use these materials for nanofiltration and desalination (*8*–*19*). GO laminates are particularly attractive because they are easy to fabricate and mechanically robust and should be amenable to industrial-scale production (*20*, *21*). They are made of impermeable functionalized graphene sheets that have a typical size of $L \approx 1$ μm and the interlayer separation, d, sufficient to accommodate a mobile layer of water (*11*–*25*). Nanometer-thick GO films have recently been tried for pressure-driven filtration, revealing promising characteristics (*15*–*18*). However, the results varied widely for different fabrication methods, and some observations relevant to the present report (permeation of large molecules) are inconsistent with the known structure of GO laminates (*20*, *21*). This suggests the presence of cracks or pin holes in those GO thin films, which obscured their intrinsic properties (*25*).

We studied micrometer-thick GO membranes prepared from GO suspensions using vacuum filtration as described in (*25*). The resulting membranes were checked for their continuity by using a helium leak detector before and after filtration experiments, which demonstrated that the membranes were vacuum-tight in the dry state (*11*). Schematics of our permeation experiments are shown in Fig. 1. The feed and permeate compartments were initially filled to the same height with different liquids, including water, glycerol, toluene, ethanol, benzene, and dimethyl sulfoxide (DMSO). No permeation could be detected over a period of many weeks by monitoring liquid levels and using chemical analysis (*25*). If both compartments were filled with water solutions, permeation through the same vacuum-tight membrane could be readily observed as rapid changes in liquid levels (several millimeters per day). For example, a level of a 1 M sucrose solution in the feed compartment rose, whereas it fell in the permeate compartment filled with deionized water. For a membrane with a thickness h of 1 μm, we found water flow rates of ≈0.2 L m^{-2} h^{-1}, and the speed increased with increasing the molar concentration C. Because a 1 M sucrose solution corresponds to an osmotic pressure of ≈25 bar at room temperature (the van't Hoff factor is 1 in this case), the flow rates agree with the evaporation rates of ≈10 L m^{-2} h^{-1} reported for similar membranes in (*11*), in which case, the permeation was driven by a capillary pressure of the order of 1000 bar. The hydrostatic pressures in our experiments never exceeded 10^{-2} bar and, therefore, could be neglected.

We next investigated the possibility that dissolved ions and molecules could diffuse through the capillaries simultaneously with water. We filled the feed compartment with various solutions to determine whether any of the solutes permeated into the deionized water on the other side of the GO membrane (Fig. 1B). As a quick test, ion transport can be probed by monitoring electrical conductivity of the permeate compartment (fig. S1). We found that for some salts (for example, NaCl), the conductivity increased with time, but for others {for example, $K_3[Fe(CN)_6]$}, it did not change over many days of measurements.

Depending on the solute, we used ion chromatography, inductively coupled plasma optical

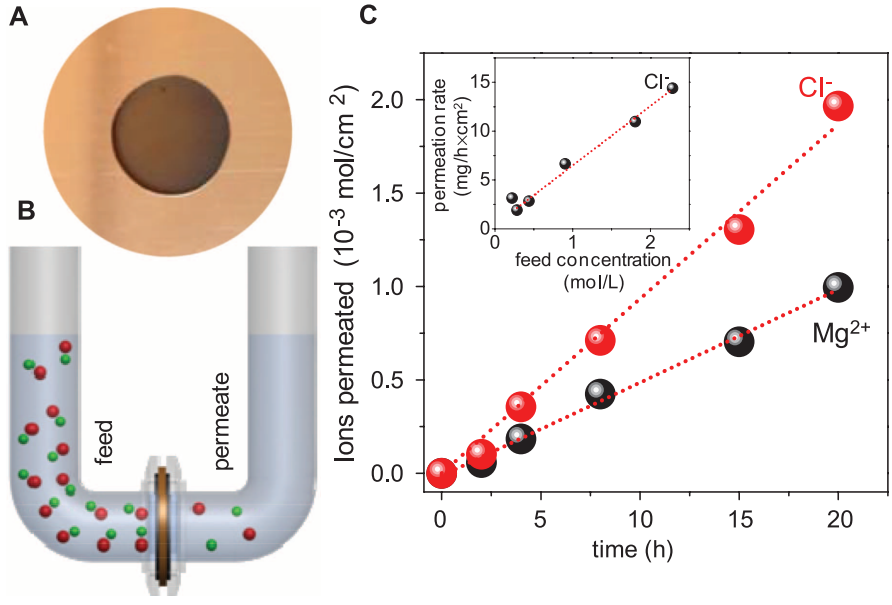

Fig. 1. Ion permeation through GO laminates. (**A**) Photograph of a GO membrane covering a 1-cm opening in a copper foil. (**B**) Schematic of the experimental setup. A U-shaped tube 2.5 cm in diameter is divided by the GO membrane into two compartments referred to as feed and permeate. Each is filled to a typical level of ~20 cm. Magnetic stirring is used so as to ensure no concentration gradients. (**C**) Permeation through a 5-μm-thick GO membrane from the feed compartment with a 0.2 M solution of $MgCl_2$. (Inset) Permeation rates as a function of C in the feed solution. Within our experimental accuracy (variations by a factor of <40% for membranes prepared from different GO suspensions), chloride rates were found the same for $MgCl_2$, KCl, and $CuCl_2$. Dotted lines are linear fits.

[1]School of Physics and Astronomy, University of Manchester, Manchester M13 9PL, UK. [2]School of Chemical Engineering and Analytical Science, University of Manchester, Manchester M13 9PL, UK. [3]Chinese Academy of Sciences Key Laboratory of Mechanical Behavior and Design of Materials, Department of Modern Mechanics, University of Science and Technology of China, Hefei, Anhui 230027, China.

*Corresponding author. E-mail: rahul.raveendran-nair@manchester.ac.uk (R.R.N.); geim@man.ac.uk (A.K.G.)

emission spectrometry, total organic carbon analysis, and optical absorption spectroscopy (*25*) to measure permeation rates for a range of molecules and ions (table S1). An example of our measurements for $MgCl_2$ is shown in Fig. 1C, using ion chromatography and inductively coupled plasma optical emission spectrometry for Mg^{2+} and Cl^-, respectively. Concentrations of Mg^{2+} and Cl^- in the permeate compartment increased linearly with time, as expected. Slopes of such curves yield permeation rates. The observed rates depend linearly on concentration in the feed compartment (Fig. 1C, inset). Cations and anions move through membranes in stoichiometric amounts so that charge neutrality within each of the compartment is preserved. For example, in Fig. 1C permeation of one Mg^{2+} ion is accompanied by two Cl^- ions, and there is no electric field buildup across the membrane.

Our results obtained for different ionic and molecular solutions are summarized in Fig. 2. The small species permeate with approximately the same speed, whereas large ions and organic molecules exhibit no detectable permeation. The effective volume occupied by an ion in water is characterized by its hydrated radius. If plotted as a function of this parameter, our data are well described by a single-valued function with a sharp cutoff at ≈4.5 Å (Fig. 2). Species larger than this are sieved out. This behavior corresponds to a physical size of the mesh of ≈9 Å. Also, permeation rates do not exhibit any notable dependence on ion charge (Fig. 2) (*12*, *13*, *23*, *26*) because triply charged ions such as AsO_4^{3-} permeate with approximately the same rate as singly charged Na^+ or Cl^-. Last, to prove the essential role of water for ion permeation through GO laminates, we dissolved KCl and $CuSO_4$ in DMSO, the polar nature of which allows solubility of these salts. No permeation was detected, confirming the special affinity of GO laminates to water.

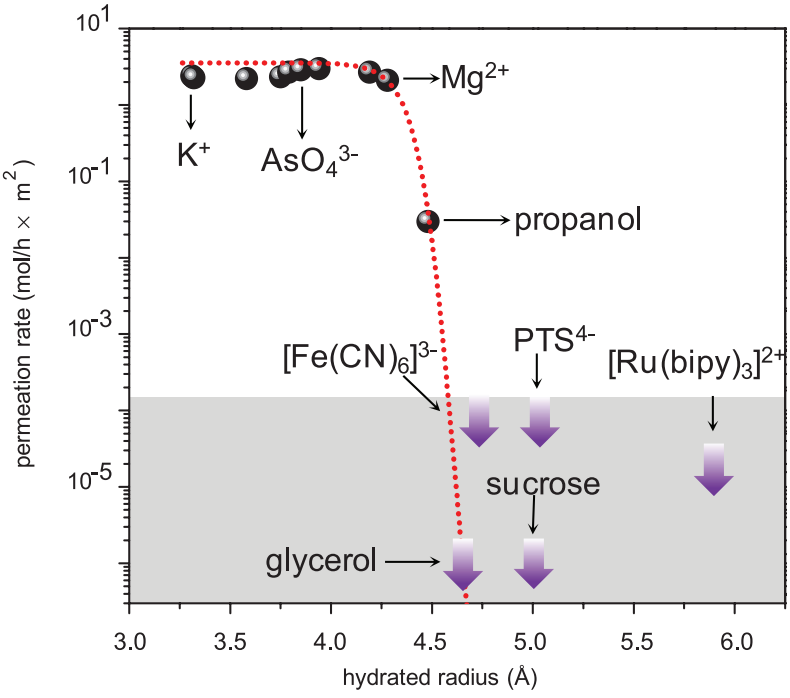

Fig. 2. Sieving through the atomic-scale mesh. The shown permeation rates are normalized per 1 M feed solution and measured by using 5-μm-thick membranes. Some of the tested chemicals are named here; the others can be found in table S1 (*25*). No permeation could be detected for the solutes shown within the gray area during measurements lasting for at least 10 days. The thick arrows indicate our detection limit, which depends on a solute. Several other large molecules—including benzoic acid, DMSO, and toluene—were also tested and exhibited no detectable permeation. The dashed curve is a guide to the eye, showing an exponentially sharp cutoff at 4.5 Å, with a width of ≈0.1 Å.

To explain the observed sieving properties, we use the model previously suggested to account for unimpeded evaporation of water through GO membranes (*11*). Individual GO crystallites have two types of regions: functionalized (oxidized) and pristine (*21*, *27*, *28*). The former regions act as spacers that keep adjacent crystallites apart and also prevent them from being dissolved. In a hydrated state, the spacers help water to intercalate between GO sheets, whereas pristine regions provide a network of capillaries that allow nearly frictionless flow of a layer of correlated water, similar to the case of water transport through carbon nanotubes (*8*–*10*). The earlier experiments using GO laminates in air (typical $d \approx 9 \pm 1$ Å) were explained by assuming one monolayer of moving water. For GO laminates soaked in water, d increases to ≈13 ± 1 Å (fig. S2), which allows two or three water layers (*19*, *22*, *23*, *29*). Taking into account the effective thickness of graphene of 3.4 Å (interlayer distance in graphite), this yields a pore size of ≈9 to 10 Å, which is in agreement with the mesh size found experimentally.

To support our model, we have used molecular dynamics (MD) simulations. The setup is shown in Fig. 3A, in which a graphene capillary separates feed and permeate reservoirs, and its width is varied between 7 and 13 Å to account for the possibility of one, two, or three layers of water (*25*). We find that the narrowest

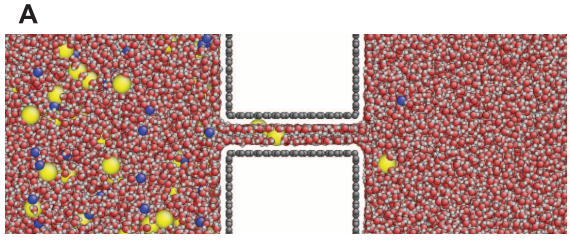

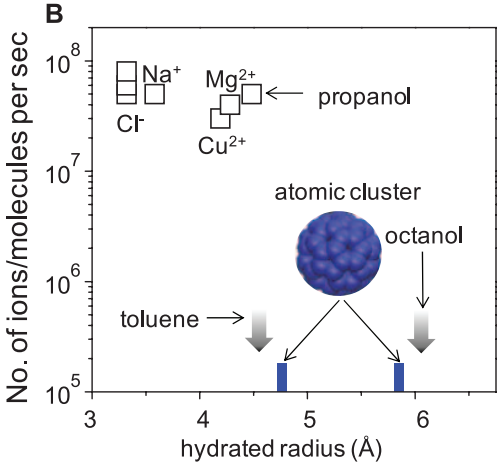

Fig. 3. Simulations of molecular sieving. (**A**) Snapshot of NaCl diffusion through a 9 Å graphene slit allowing two layers of water. Na^+ and Cl^- ions are in yellow and blue, respectively. (**B**) Permeation rates for NaCl, $CuCl_2$, $MgCl_2$, propanol, toluene, and octanol for such capillaries. For octanol poorly dissolved in water, the hydrated radius is not known, and we use its molecular radius. Blue marks indicate permeation cutoff for an atomic cluster (inset) for graphene capillaries accommodating two and three layers of water (widths of 9 and 13 Å, respectively).

capillaries become filled with a monolayer of water as described previously (*11*) and do not allow even such small ions as Na^+ and Cl^- inside. However, for two and three layers expected in the fully hydrated state (*25*) ions enter the capillaries and diffuse into the permeate reservoir. Their diffusion rates are found to be approximately the same for all small ions and show little dependence on ionic charge (Fig. 3B). Larger species (toluene and octanol) cannot permeate even through capillaries containing three layers of water (fig. S3). We have also modeled large solutes as atomic clusters of different size (*25*) and found that the capillaries accommodating two and three layers of water rejects clusters with the radius larger than ≈4.7 and 5.8 Å, respectively. This may indicate that the ion permeation through GO laminates is limited by regions containing two layers of water. The experimental and theory results in Figs. 2 and 3B show good agreement.

Following (*11*), we estimate that for our laminates with $h \approx 5$ μm and $L \approx 1$ μm, the effective length of graphene capillaries is $L \times h/d \approx 5$ mm and that they occupy $d/L \approx 0.1\%$ of the surface area. This estimate is supported by measuring the volume of absorbed water, which is found to match the model predictions (*25*). For a typical diffusion coefficient of ions in water ($\approx 10^{-5}$ cm^2 s^{-1}), the expected diffusion rate for a 1 M solution through GO membrane is $\approx 10^{-3}$ mol h^{-1} m^{-2} (*25*)—that is, several thousands of times smaller than the rates observed experimentally (Fig. 1C). Such fast transport cannot be explained by the confinement, which increases the diffusion coefficient by only a factor of 3/2, reflecting the change from bulk to two-dimensional water. Moreover, functionalized regions [modeled as graphene with randomly attached epoxy and hydroxyl groups (*20*, *21*)] do not enhance diffusion but rather suppress it (*25*, *29*) as expected because of the broken translational symmetry.

To understand the ultrafast ion permeation, we recall that graphite-oxide powders exhibit extremely high absorption efficiency with respect to many salts (*30*). Despite being densely stacked, our GO laminates are found to retain this property for salts with small hydrated radii [(*25*), section 6]. Our experiments show that permeating salts are absorbed in amounts reaching as much as 25% of the membrane's initial weight (fig. S2). The large intake implies highly concentrated solutions inside graphene capillaries (close to the saturation). Our MD simulations confirm that small ions prefer to reside inside capillaries (fig. S4). The affinity of salts to graphene capillaries indicates an energy gain with respect to the bulk water, and this translates into a capillary-like pressure that acts on ions within a water medium (*25*). Therefore, there is a large capillary force, sucking small ions inside GO laminates and facilitating their permeation. Our MD simulations provide an estimate for this ionic pressure as >50 bars (*25*).

The reported GO membranes exhibit extraordinary separation properties, and their full understanding will require further work both experimental and theoretical. With the ultrafast ion transport and atomic-scale pores, GO membranes already present an interesting material to consider for separation and filtration technologies, particularly those that target extraction of valuable solutes from complex mixtures. By avoiding the swelling of GO laminates in water (by using mechanical constraints or chemical binding), it may be possible to reduce the mesh size down to ~6 Å; in which case, one monolayer of water would still go through, but even the smallest salts would be rejected.

References and Notes

1. K. B. Jirage, J. C. Hulteen, C. R. Martin, *Science* **278**, 655–658 (1997).
2. N. B. McKeown, P. M. Budd, *Chem. Soc. Rev.* **35**, 675–683 (2006).
3. D. L. Gin, R. D. Noble, *Science* **332**, 674–676 (2011).
4. D. Cohen-Tanugi, J. C. Grossman, *Nano Lett.* **12**, 3602–3608 (2012).
5. S. P. Koenig, L. Wang, J. Pellegrino, J. S. Bunch, *Nat. Nanotechnol.* **7**, 728–732 (2012).
6. M. Ulbricht, *Polymer (Guildf.)* **47**, 2217–2262 (2006).
7. M. Elimelech, W. A. Phillip, *Science* **333**, 712–717 (2011).
8. J. K. Holt *et al.*, *Science* **312**, 1034–1037 (2006).
9. M. Majumder, N. Chopra, R. Andrews, B. J. Hinds, *Nature* **438**, 44 (2005).
10. G. Hummer, J. C. Rasaiah, J. P. Noworyta, *Nature* **414**, 188–190 (2001).
11. R. R. Nair, H. A. Wu, P. N. Jayaram, I. V. Grigorieva, A. K. Geim, *Science* **335**, 442–444 (2012).
12. M. Majumder, N. Chopra, B. J. Hinds, *J. Am. Chem. Soc.* **127**, 9062–9070 (2005).
13. F. Fornasiero *et al.*, *Proc. Natl. Acad. Sci. U.S.A.* **105**, 17250–17255 (2008).
14. L. Qiu *et al.*, *Chem. Commun. (Camb.)* **47**, 5810–5812 (2011).
15. P. Sun *et al.*, *ACS Nano* **7**, 428–437 (2013).
16. Y. Han, Z. Xu, C. Gao, *Adv. Funct. Mater.* **23**, 3693–3700 (2013).
17. M. Hu, B. Mi, *Environ. Sci. Technol.* **47**, 3715–3723 (2013).
18. H. Huang *et al.*, *Chem. Commun. (Camb.)* **49**, 5963–5965 (2013).
19. K. Raidongia, J. Huang, *J. Am. Chem. Soc.* **134**, 16528–16531 (2012).
20. D. A. Dikin *et al.*, *Nature* **448**, 457–460 (2007).
21. G. Eda, M. Chhowalla, *Adv. Mater.* **22**, 2392–2415 (2010).
22. A. Lerf *et al.*, *J. Phys. Chem. Solids* **67**, 1106–1110 (2006).
23. D. W. Boukhvalov, M. I. Katsnelson, Y.-W. Son, *Nano Lett.* **13**, 3930–3935 (2013).
24. S. You, S. M. Luzan, T. Szabó, A. V. Taluzin, *Carbon* **52**, 171–180 (2013).
25. Materials and methods are available as supplementary materials on *Science* Online.
26. B. Van der Bruggen, J. Schaep, D. Wilms, C. Vandecasteele, *J. Membr. Sci.* **156**, 29–41 (1999).
27. N. R. Wilson *et al.*, *ACS Nano* **3**, 2547–2556 (2009).
28. D. Pacilé *et al.*, *Carbon* **49**, 966–972 (2011).
29. N. Wei, Z. Xu, Breakdown of fast water transport in graphene oxides. arXiv:1308.5367.
30. S. Wang, H. Sun, H. M. Ang, M. O. Tade, *Chem. Eng. J.* **226**, 336–347 (2013).

Acknowledgments: This work was supported by the European Research Council, the Royal Society, Engineering and Physical Research Council (UK), and the National Natural Science Foundation (China). We thank A. Mishchenko and J. Waters for help. R.K.J. also acknowledges support by the Marie Curie Fellowship, and R.R.N. acknowledges support by the Leverhulme Trust and Bluestone Global Tech.

Supplementary Materials

www.sciencemag.org/content/343/6172/752/suppl/DC1
Materials and Methods
Figs. S1 to S4
Table S1
References (*31*–*52*)

9 September 2013; accepted 9 January 2014
10.1126/science.1245711

Designing Collective Behavior in a Termite-Inspired Robot Construction Team

Justin Werfel,[1]* Kirstin Petersen,[1,2] Radhika Nagpal[1,2]

Complex systems are characterized by many independent components whose low-level actions produce collective high-level results. Predicting high-level results given low-level rules is a key open challenge; the inverse problem, finding low-level rules that give specific outcomes. We present a multi-agent construction system inspired by mound-building termites, solving such an inverse problem. A user specifies a desired structure, and the system automatically generates low-level rules for independent climbing robots that guarantee production of that structure. Robots use only local sensing and coordinate their activity via the shared environment. We demonstrate the approach via a physical realization with three autonomous climbing robots limited to onboard sensing. This work advances the aim of engineering complex systems that achieve specific human-designed goals.

In contrast to the careful preplanning and regimentation that characterize human construction projects, animals that build in groups do so in a reactive and decentralized way. The most striking examples are mound-building termites, colonies of which comprise millions of independently behaving insects that build intricate structures orders of magnitude larger than themselves (*1*, *2*) (Fig. 1, A and B). These natural systems inspire us to envision artificial ones operating via similar principles (*3*, *4*), with independent agents

[1]Wyss Institute for Biologically Inspired Engineering, Harvard University, Cambridge, MA 02138, USA. [2]School of Engineering and Applied Sciences, Harvard University, Cambridge, MA 02138, USA.
*Corresponding author. E-mail: justin.werfel@wyss.harvard.edu